

# Brane Mechanics

R. Abbaspur<sup>1</sup>

*Institute for Studies in Theoretical Physics and Mathematics,  
P.O. Box 19395-5531, Tehran, Iran.  
Department of Physics, Sharif University of Technology,  
P. O. Box 19365-9161, Tehran, Iran.*

## Abstract

In this paper, we investigate about two physically distinct classes of the ‘one-dimensional’ worldvolume solutions describing the status of an arbitrary brane in the presence of another arbitrary (flat) brane which supplies the required supergravity background. One of these classes concerns with a relative (transverse) motion of two parallel flat branes, while the other class is related to a static configuration in which one of the branes is flat and the other is curved as a cylindrical hypersurface. Global symmetries of the worldvolume theory are used to show that both types of these solutions are described by some sort of ‘planar orbits’ which are specified by their ‘energy’ and ‘angular momentum’  $(E, l)$  parameters. We find that various phases of the ‘motion’ along these orbits, for different values of  $(E, l)$ , are easily deduced from the curve of an  $E$ -dependent function of the relative ‘distance’ between the two branes, which is somehow related to their mutual ‘effective potential’.

---

<sup>1</sup>e-mail:abbaspur@netware2.ipm.ac.ir

# 1 Introduction

The description of the composite systems of branes [1, 2, 3] in terms of the source and probe (S,P) configurations has proved itself as a useful technique for investigating about some of the features of the intersecting brane configurations [4, 5, 6]. As has been analyzed in [4], describing a system of branes in this manner, one can find a subset of the ‘field constraints’ (the no-force conditions) that fix the supergravity solution for a ‘marginal’ configuration of ‘flat’ intersecting or overlapping branes. Moreover, by this analysis several ‘algebraic constraints’, arising naturally as the ‘consistency conditions’ in the study of the supergravity field equations, acquire interpretations as the conditions for balancing several internal long-range forces against each other. Equivalently, one can interpret them as the balancing conditions for the forces acting between the whole of the brane system and external brane probes of different types and orientations similar to those of the brane system [4]. A similar approach in systems of branes at angles reveals that the only *marginal* configurations with flat branes at (non-trivial) angles are those constructed from similar branes with two angles in a subgroup of  $SU(2)$  [7]. From the viewpoint of the supergravity theory, these configurations preserve 1/4 of the spacetime SUSY [8, 9]. There exist, however, other configurations of intersecting branes making more than two angles, but still preserve some fraction of SUSY [8, 10]. These configurations are stable only when certain relations (which embody the above  $SU(2)$  relation) hold between their angles [10, 11]. Such configurations, are found in [7] that, can not be made up of a set of flat p-branes. Indeed, they consist of a set of curved p-branes which only asymptotically look like the flat intersecting (overlapping) branes with definite angles. This agrees with a result of [12] that the supergravity solutions for the *non-orthogonal* intersecting branes of the distributed type at *non*  $SU(2)$  angles are not realizable in terms of a set of harmonic functions. However, the existence of such ‘curved intersections’ raises the question of finding the corresponding worldvolume solutions. This generally defines a difficult problem which involves solving simultaneously the coupled set of the supergravity and the worldvolumes field equations. As everybody knows, even the much simpler but analogous problem for two charged particles in a flat spacetime has not an exact solution. In a limiting case, however, the problem is simplified and can be handled using the S-P description. This is the viewpoint that we shall follow in this paper to study a special class of the curved configurations which we name as the ‘mono-dimensional’ solutions. The organization of the paper is as follows: The general set up of the problem together with the required notations are given in section 2. Then in section 3, the symmetries of the worldvolume theory and its Noether currents, in connection to a class of its solutions named as the ‘orbits’, are studied. Sections 4,5,6 are devoted to a detailed analysis of the orbits in three different cases of the source and probe dimensions on the basis of the conservation

equations given in section 3. The paper ends with some concluding remarks in section 7.

## 2 Some general remarks

The basic principle in the analysis of any system of (S,P)-branes (as the source and probe respectively) is that, while the worldvolume geometry of the P-brane is essentially determined by the fields that originate from the S-brane, the latter is not influenced in any way by the presence of the former. In analogy to classical mechanics, such a condition corresponds to a limiting case in which one of the branes, labeled by S, has a considerable mass relative to the other brane which is labeled by P. In the case of BPS (1/2 SUSY) branes, one knows that each of the branes has a mass and charge in proportion to its tension  $T_s$  or  $T_p$  [5]; so in suitable units one must require that  $T_s \gg T_p$ . There are other occasions, however, that while this condition on tensions is not necessarily satisfied, the description as a (S,P) system still is reliable. An interesting example of such occasions is a marginally bound BPS configuration of two flat p-branes which are characterized by certain no-force conditions among themselves [4, 5, 13]. In general, a BPS-brane with a small (extrinsic) curvature in the background of another such flat brane, both together, can be treated (in this same order) as a pair of (P,S)-branes. Another application concerns the near to the intersection points of two p-branes where one can neglect the self-interactions of each brane in comparison to its interactions with the other brane. In usual, a flat p-brane of the BPS type is a classically stable object, which obeys certain no-force conditions preventing its collapse due to its self-gravitational forces. When the p-brane is curved, the self-interaction forces counterbalance each other and the oscillations initiate. In a S-P description, however, we deal with a limiting case in which all of the ‘self-oscillations’ of the P-brane, as well as its curving effects on the geometry of the S-brane, are totally negligible. As a result, the analysis for a S-P configuration with a pair of BPS-branes proceeds via studying the worldvolume (DBI+WZ) action of the P-brane, in which the background fields are replaced by the fields associated to a flat and fixed S-brane. In general, the analysis depends on the ‘types’ of the two branes which-as far as concerns to us- are specified by their dimensions, ‘electric’ or ‘magnetic’ nature and couplings to the dilaton field. For the purpose of this paper we restrict our study to the case with both electric-type (S,P)-branes and distinguish between several cases by the relative status of the worldvolume dimensions  $(d_s, d_p)$  of these two branes.

To begin with, we recall that the general supergravity background for a (BPS)  $(d - 1)$ -brane source consists of [5, 6]

$$ds^2 = H^{d/\bar{D}}(H^{-1}\eta_{\mu\nu}dx^\mu dx^\nu + \delta_{mn}dy^m dy^n)$$

$$e^\phi = H^\alpha$$

$$\mathcal{A} = H^{-1} \Lambda_{\mu=0}^{d-1} dx^\mu \quad (1)$$

Here  $x^\mu$  and  $y^m$  are parallel and transverse coordinates of the S-brane, and  $H$  is a harmonic function:

$$H(y) = \begin{cases} 1 + Q/|y|^{\tilde{d}} & , \quad \tilde{d} \neq 0 \\ -Q \ln |y| & , \quad \tilde{d} = 0 \end{cases} \quad (2)$$

where  $|y|^2 = y^m y^m$  and  $Q$  is (proportional to) the form-field charge of the brane. All other notations are those of [4], in particular:  $\bar{D} := D - 2$ ,  $\tilde{d} := \bar{D} - d$ ,  $D$  is the spacetime dimension and  $\alpha$  is a measure of coupling between  $\phi$  and  $\mathcal{A}$  in supergravity, which is related to  $d$  as: [5, 6]

$$\alpha^2(d) = 1 - d\tilde{d}/2\bar{D} \quad (3)$$

On the other hand the worldvolume action for a  $(d - 1)$ -brane probe (having equal mass and charge in units with  $16\pi G_D = 1$ ) has the general form [5, 14]:

$$S_d = -T_d \int d^d \xi e^{-\alpha\phi} \det^{1/2}(g_{ab}^*) + T_d \int \mathcal{A}_{(d)}^* \quad (4)$$

where  $g_{ab}^*$  and  $\mathcal{A}^*$  are pull-backs of the spacetime metric and the  $d$ -form potential, on the  $d$ -volume of the probe, respectively. Depending on that  $d_s = d_p$  or  $d_s \neq d_p$ , the last (WZ) term has a non-vanishing or vanishing contribution to  $S_d$ . This action describes the dynamics of the embedding coordinates  $X^M = X^M(\xi)$  through the dependences of  $\phi, g_{ab}^*, \mathcal{A}^*$  on these coordinates. In the following sections, however, we use a subset ( $x^a$ ) of the spacetime coordinates ( $x^M$ ) (parallel or perpendicular to the source) to parameterize the worldvolume of the P-brane and use the remaining subset ( $y^A$ ) as the embedding coordinates [so,  $(x^a, y^A) \equiv (x^\mu, y^m)$ ]. The above action then reads

$$S_d = T_d \int d^d x \mathcal{L}(Y^A, \partial_a Y^A) \quad (5)$$

where the form of the embedding Lagrangian ( $\mathcal{L}$ ) changes depending on the relative status of  $d_s$  and  $d_p$  (see below).

### 3 Symmetries of $\mathcal{L}$ and the orbits

Without going to the detailed expression of  $\mathcal{L}$  in the specific cases, the flat geometry of the S-brane a priori implies that this Lagrangian must possess a number of obvious global symmetries. These symmetries include the translational and rotational invariances along the worldvolume of the S-brane as well as the rotational invariance along its transverse directions which are respectively defined as:

$$\delta x^\mu = \varepsilon^\mu \quad , \quad \delta y^m = 0 \quad (6)$$

$$\delta x^\mu = \lambda_\nu^\mu x^\nu \quad , \quad \delta y^m = 0 \quad (\lambda_{\mu\nu} + \lambda_{\nu\mu} = 0) \quad (7)$$

$$\delta x^\mu = 0 \quad , \quad \delta y^m = \omega_{mn} y^n \quad (\omega_{mn} + \omega_{nm} = 0) \quad (8)$$

Though all of these symmetries have natural interpretations as the spacetime (bulk) symmetries, in the worldvolume theory some of them are realized as pure internal symmetries changing  $Y^A(x^a)$ 's but not affecting on  $x^a$ . The three cases with  $d_s \Leftrightarrow d_p$  are common in the above symmetries, though they are different in the way that one defines  $(x^a, y^A)$ . In each of the above cases they are defined as follows:

$$\begin{aligned}
d_s = d_p & : & x^\mu = x^a & , & y^m = y^A \\
d_s > d_p & : & x^\mu = (x^a, y^i) & , & y^m = y^A \\
d_s < d_p & : & x^a = (x^\mu, y^i) & , & y^m = (y^A, y^i)
\end{aligned} \tag{9}$$

Here  $(y^i)$  represents a subset of the coordinates parallel (perpendicular) to the S-brane which we shall take them as a part of the parameterizing (embedding) coordinates, in the case with  $d_s > d_p$  ( $d_s < d_p$ ). The corresponding Noether currents for each of these cases are then constructed using the formula [15]:

$$\mathcal{J}^a = \frac{\partial \mathcal{L}}{\partial Y_{,a}^A} (\delta Y^A - \delta x^b \partial_b Y^A) + \mathcal{L} \delta x^a \tag{10}$$

The conservation equations of the Noether currents are useful tools in the analysis of the classical solutions of the worldvolume theory (5) for a particular class of them depending only on a single space or time coordinate. For the reason that becomes clear, we refer to such solutions as the ‘orbits’ of the P-brane and denote by  $x$  the space or time coordinate that parameterizes an orbit. For such a configuration, the action (5) for the worldvolume field theory reduces to a mechanical type action of the form

$$S = \int dx L(Y^A, \dot{Y}^A) \tag{11}$$

where  $Y^A = Y^A(x)$ ,  $\dot{Y}^A := dY^A/dx$ , and  $L(Y^A, \dot{Y}^A)$  (up to a constant factor) is the same as  $\mathcal{L}(Y^A, \partial_a Y^A)$  in which all derivatives of  $Y^A$  other than  $\dot{Y}^A$  are set equal to zero. Depending on that  $x$  is a space- or time-like coordinate the resulting solution has a different interpretation. When  $x$  is space-like,  $Y^A(x)$  describes a cylindrical static configuration of the P-brane, whose all directions except one are parallel to the S-brane. When  $x$  is time-like,  $Y^A(x)$  describes the path of the motion for a P-brane remaining parallel to a S-brane and moving transverse to it. In the subspace transverse to all of the  $x^a$  directions, the configuration (of the P-brane) defined by  $Y^A = Y^A(x)$  is projected into a curve which looks like the orbit of a point particle moving within a spherically symmetric potential. The adjective ‘space- (time-)like’ for the orbits then signifies that the corresponding curve in the subspace of  $(x, y^A)$  is space- (time-)like, meaning that  $x$  itself is a space- (time-)like coordinate. For both classes of such *mono-dimensional* solutions, the equations of motion of (11) can be more easily integrated using a set of

conservation laws corresponding to the symmetries given by (6)-(8). Generically, for an orbit depending on  $x$ , a conservation law as  $\partial_a \mathcal{J}^a = 0$  yields

$$\frac{d\mathcal{J}^x}{dx} = 0 \quad (12)$$

which identifies the component  $\mathcal{J}^x$  of the current as a conserved charge along the orbit. We will see in the following sections that these conserved charges provide the sufficient information required for integrating the equations of motion for  $Y^A(x)$ . Then we observe that the orbits are effectively characterized by the 2-dimensional motion of a point particle in the Newtonian mechanics whose different phases of motion are determined by an effective potential depending on two (energy and angular momentum) parameters. The analysis then proceeds via a set of (phase) diagrams depending only on the energy parameter, and reveals a variety of regimes (phases of the effective motion) for orbits with various parameters. We study the three cases with  $d_s \Leftrightarrow d_p$  through separate analyses in the next three sections.

## 4 The S-P system with $d_s = d_p$

In this case the 1<sup>st</sup> row of (9) defines  $(x^a, y^A)$  and the Lagrangian  $\mathcal{L}$ , using eqs.(1)-(4), for a general configuration is written as

$$\mathcal{L} = -H^{-1}(Y)[\det^{1/2}(\delta_\nu^\mu + H(Y)\partial^\mu Y^m \partial_\nu Y^m) - \eta] \quad (13)$$

where  $\eta = +1(-1)$  for a brane-brane (brane-anti-brane) S-P configuration (note that in this case the two branes ‘see’ the form-fields of each other via a force depending on their relative orientation; the sign of  $\eta$  reflects this orientation). The conserved currents in this case consist of:

$$T_\nu^\mu = \frac{\partial \mathcal{L}}{\partial Y_{,\mu}^m} Y_{,\nu}^m - \delta_\nu^\mu \mathcal{L} \quad , \quad \partial_\mu T^{\mu\nu} = 0 \quad (14)$$

$$M^{\mu\nu\rho} = x^\rho T^{\mu\nu} - x^\nu T^{\mu\rho} \quad , \quad \partial_\rho M^{\mu\nu\rho} = 0 \quad (15)$$

$$J_{mn}^\mu = Y^m \frac{\partial \mathcal{L}}{\partial Y_{,\mu}^n} - Y^n \frac{\partial \mathcal{L}}{\partial Y_{,\mu}^m} \quad , \quad \partial_\mu J_{mn}^\mu = 0 \quad (16)$$

which in correspondence to the symmetries (6)-(8) have to be identified as the energy-momentum, ‘longitudinal’ and ‘transverse’ angular momentum tensors respectively. Since the conservation of  $M^{\mu\nu\rho}$  naturally follows from that of  $T^{\mu\nu}$ , only the eqs.(14) and (16) are taken as the informative parts of the conservation laws for this analysis. Going to the mono-dimensional solutions, the Lagrangian (13) becomes

$$L = -H^{-1}[(1 + \varepsilon H \dot{Y}^2)^{1/2} - \eta] \quad (17)$$

where  $\varepsilon = +1(-1)$ , if  $x$  is a space- (time-)like coordinate and  $\dot{Y}^2 := \dot{Y}^m \dot{Y}^m$ . The corresponding conserved charges, according to eqs.(12),(14),(16), are

$$E = \dot{Y}^m \frac{\partial L}{\partial \dot{Y}^m} - L = -H^{-1} \left( \eta - \frac{1}{\sqrt{1 + \varepsilon H \dot{Y}^2}} \right) \quad (18)$$

$$J^{mn} = \dot{Y}^m \frac{\partial L}{\partial \dot{Y}^n} - \dot{Y}^n \frac{\partial L}{\partial \dot{Y}^m} = -\frac{\varepsilon(Y^m \dot{Y}^n - Y^n \dot{Y}^m)}{\sqrt{1 + \varepsilon H \dot{Y}^2}} \quad (19)$$

For a time-like orbit ( $\varepsilon = -1$ ),  $E$  and  $J^{mn}$  have obvious interpretations as the energy <sup>2</sup> and the (transverse) angular momentum tensor (of the P-brane) respectively. For a space-like orbit ( $\varepsilon = +1$ ), however, they have to be interpreted as the flows of the respective quantities along the orbit ( $x$ ) direction <sup>3</sup>.

As in the ordinary 3D particle mechanics, one expects that the angular momentum conservation restricts the dimension of the orbits (hyper)planes. Such a property is in fact a result of the equation(s) obtained from eq.(19) by eliminating the velocities; that is

$$J^{mn} Y^p + J^{np} Y^m + J^{pm} Y^n = 0 \quad (20)$$

where distinguished equations are obtained for distinct values of  $m, n, p = 1, \dots, M$  with  $M := \tilde{d}_s + 2$ . So, the orbit  $Y^m = Y^m(x)$  lies at the common intersection of a set of  $(M - 1)$ -dimensional hyperplanes defining the ‘orbit plane’. The (maximum) number of independent equations of the form eq.(20) thus fixes the (maximum) dimension of the orbit plane. For  $M > 3$  one can show that this plane, just as in the Newtonian particle mechanics, is a 2-dimensional plane, provided <sup>4</sup>

$$J^{12} J^{34} + J^{13} J^{42} + J^{14} J^{23} = 0, \quad \text{etc.} \quad (21)$$

Further, when (all)  $J^{mn} = 0$ , the orbit plane degenerates to a straight line or a single point. By rotating the  $y^m$  coordinates, so that the orbit plane coincides with the  $y^1 y^2$ -plane, all  $J^{mn}$ ’s except  $J^{12}$  are transformed to zero (obviously, such  $J^{mn}$ ’s obey eq.(21)). Using the polar coordinates  $(r, \theta)$  in the  $y^1 y^2$ -plane, the conservation laws (18),(19) will read

$$\frac{1}{H(r)} \left( -\eta + \frac{1}{\sqrt{1 + \varepsilon H(r) (\dot{r}^2 + r^2 \dot{\theta}^2)}} \right) = E \quad (22)$$

---

<sup>2</sup>This is indeed the *binding* energy of the configuration in units of the source tension  $T_s$ , which excludes the rest masses of (S,P)-branes.

<sup>3</sup>It is easy to check that in both cases  $T^\mu_\nu$  is a diagonal matrix, with  $T^x_x = E$  and its all other diagonal components are equal to  $(-L)$ . So, for  $\varepsilon = -1$ ,  $E$  is the energy while for  $\varepsilon = +1$  it is a component of the (anisotropic) pressure along the  $x$  direction.

<sup>4</sup>For  $M = 1, 2, 3$ , one have respectively 0,1,3 non-zero components for  $J^{mn}$  and a relation of the type of eq.(21) is not required.

$$\frac{r^2 \dot{\theta}}{\sqrt{1 + \varepsilon H(r)(\dot{r}^2 + r^2 \dot{\theta}^2)}} = l \quad (23)$$

where  $H(r)$  is the same as  $H(y)$  (eq.(2)) with  $r \equiv |y|$ , and  $l := -\varepsilon J^{12}$  is the angular momentum parameter. Solving these two eqs.for  $(\dot{r}, \dot{\theta})$ , one obtains

$$\dot{r}^2 = U(r) := \frac{-2\varepsilon\eta E - \varepsilon E^2 H - l^2/r^2}{(\eta + EH)^2} \quad (24)$$

$$\dot{\theta} = \omega(r) := \frac{l/r^2}{\eta + EH(r)} \quad (25)$$

These two equations, in principle, determine the orbit up to the integrations

$$x = \pm \int^r \frac{ds}{\sqrt{U(s)}} \quad (26)$$

$$\theta = \pm \int^r ds \frac{\omega(s)}{\sqrt{U(s)}} \quad (27)$$

where the choice of the  $+$  ( $-$ ) sign corresponds to an incoming (outgoing) effective radial motion. Solving eqs. (26),(27) for  $(r(x), \theta(x))$  then specifies the form of the projection of the P-brane as a 3D curve in the  $(x, y^1, y^2)$  subspace. However, the shape of the orbit in the  $y^1 y^2$ -plane can be directly determined by solving a differential equation, obtained from eqs.(24),(25), as

$$\left(\frac{dr}{d\theta}\right)^2 = \frac{U(r)}{\omega^2(r)} = \frac{r^2}{l^2}[f(r) - l^2] \quad (28)$$

where  $f(r)$  is defined in terms of  $H(r)$  as

$$f(r) := -\varepsilon r^2 [2\eta E + E^2 H(r)] \quad (29)$$

In terms of this function,  $U(r)$  and  $\omega(r)$  (eqs.(24),(25)) are expressed as

$$U(r) = \frac{E^2 r^2 (f(r) - l^2)}{(f(r) + \varepsilon \eta E r^2)^2} \quad (30)$$

$$\omega(r) = \frac{\varepsilon l E}{f(r) + \varepsilon \eta E r^2} \quad (31)$$

## 4.1 The effective one-dimensional motion

eq.(24) is similar to an energy conservation equation for the 1-dimensional (radial) motion of a point particle within an external force field derivable from the potential  $-\frac{1}{2}U(r)$  and with  $x$  identified as the time variable. Except for a few examples, explicit integration of this equation for  $r(x)$  is generally impossible. However, as in many other dynamical systems, the qualitative behavior of the solution and its different phases are distinguishable



from a set of ‘phase diagrams’; i.e. the curves describing the motion in the  $(r, \dot{r})$  plane. These curves are, in effect, the symmetrized version of the  $U(r)$  diagrams for different values of the  $(E, l)$  parameters. However, a more simplified discussion of the effective motion proceeds via studying the diagrams for  $f(r)$  which are dependent only on the  $E$  parameter. The expression of eq.(30) for  $U(r)$  shows that the allowed region of the ‘effective radial motion’ are specified by the values of  $r$  satisfying the inequality

$$U(r) \geq 0 \quad \equiv \quad f(r) \geq l^2 \quad (32)$$

Within every connected region of  $r$  with this property, the ‘effective particle’ moves in a definite direction (depending on the sign in eq.(26)) under the radial force  $\frac{1}{2}U'(r)$ , until it reaches to an end-point of the interval, where its velocity vanishes and (provided the force is still non-vanishing) reverses its direction. Obviously, such ‘turning points’ are defined by

$$f(r_0) = l^2 \quad , \quad f'(r_0) \neq 0 \quad (33)$$

In addition, the positivity of the square root in in eq.(22) requires that

$$\eta + EH(r) > 0 \quad (34)$$

By eq.(25), this result implies that the angular ‘velocity’  $\omega(r)$  has a definite sign (depending on  $l$ ), which is an indication of a *monotonic* angular ‘motion’ around the origin. By eqs.(2) and (29), the explicit expression for  $f(r)$  is

$$f(r) = \begin{cases} \varepsilon(ar^2 - b/r^{M-4}) & , \quad M \neq 2 \\ \varepsilon(cr^2 + br^2 \ln r) & , \quad M = 2 \end{cases} \quad (35)$$

where the various parameters are defined as<sup>5</sup>:

$$a := -2\eta E - E^2 \quad , \quad b := E^2 Q \quad , \quad c := -2\eta E \quad (36)$$

For each specific situation (i.e. a case with a specific  $M, \varepsilon, \eta$ ), fixing the energy  $E$  of the P-brane specifies the shape of the graph for  $f(r)$ . Changing  $l^2$ , as the height of a horizontal line on this graph, then according to eq.(32), specifies various allowed regimes of the effective motion. Evidently, in all cases that  $f(r) \equiv 0$  ( $\forall r \geq 0$ ), one necessarily has  $l = 0$  and in such a case any *constant* values of  $(r, \theta)$  specify a solution of the equations of motion. Such a solution, which is the same as a multi-center solution for two parallel branes, can be formed at any arbitrary separation of the two branes thereby defining a *marginal* configuration [6, 3]. By eqs.(35),(36), such a configuration is only achieved for  $E = 0$ , i.e. for a zero binding energy. This is the only configuration of two similar branes in the desired category which is marginal and preserves a 1/2 SUSY fraction.

---

<sup>5</sup>Note to the dimensionality of the parameters as:  
 $E \sim (\text{length})^0 \quad l \sim (\text{length})^1 \quad Q \sim (\text{length})^{M-2}$

## 4.2 Qualitative description of the orbits

The following qualitative descriptions are deduced from the inspection of the the graphs of  $f(r)$  in Fig.(1), which are sketched for the space-like orbits, and those for the time-like orbits which are obtained by reversing these graphs (not shown). The parameter  $a$  in these diagrams is related to the energy parameter  $E$  as in the eq.(36).

### *Space-like orbits ( $\varepsilon = +1$ )*

For all the transverse dimensions  $M \geq 3$ , these orbits share the common feature that, for all values of  $l$ , they have extensions to the infinite region  $r \rightarrow \infty$  and pass through a minimum distance ( $r_0$ ) relative to the source. They are all symmetric around their minimum points and make a finite angle ( $\gamma$ ) with respect to the  $x$  direction (see below). All of these ‘solitons’ are stable only for those combinations of  $(E, \eta)$  that leave  $a > 0$ . For  $M = 1$ , which normally has  $l = 0$ , the orbit crosses the source (at  $r = 0$ ) and passes through a maximum distance ( $r_0$ ) and oscillates periodically along the  $x$  direction. The stability in this case is also achieved for  $a > 0$ . The  $M = 2$  case is distinguished by the fact that the coordinate  $r$  possesses a natural bound  $r \leq 1$  so that  $H(r) \geq 0$  and the transverse part of the metric remains positive. The corresponding orbits then oscillate between  $r_0 \leq r \leq 1$ , and are stable provided  $c > 0$  (so that  $r_0 < 1$ ).

### *Time-like orbits ( $\varepsilon = -1$ )*

Unlike the space-like case, time-like diagrams in all of the three branches with  $a \leq 0$  possess allowable regimes of ‘motion’. Possible regimes are:

$M \geq 5$  ,  $a \geq 0$  : For all  $l^2 \geq 0$  the orbit is bound between  $0 \leq r \leq r_0$ , though for  $a = 0$  ,  $l = 0$  it extends to infinity:  $0 \leq r < \infty$ .

$M \geq 5$  ,  $a < 0$  : There is a critical value  $l_0^2$ , so that the orbits with  $l^2 < l_0^2$  range between  $0 \leq r < \infty$ , while for  $l^2 \geq l_0^2$  two different regimes in:  $0 \leq r \leq r_1$  and  $r \geq r_2$  with the same amounts of  $(E, l)$  are equally possible.

$M = 4$  ,  $a > 0$  : For each  $l^2 \leq l_0^2$ , the orbit is bound between  $0 \leq r \leq r_0$ . Larger values of  $l^2$  are not allowable.

$M = 4$  ,  $a < 0$  : For each  $l^2 \leq l_0^2$  the orbit ranges in  $0 \leq r < \infty$ , while for  $l^2 > l_0^2$  it ranges in  $r \geq r_0$ .

$M = 4$  ,  $a = 0$  : For all  $l^2 < l_0^2$ , the orbit is a spiral between  $0 < r < \infty$ . For the critical value  $l^2 = l_0^2$ , it becomes a circle of *arbitrary* radius which is traversed with a constant angular velocity.

$M = 3$  ,  $a > 0$  : For all  $l^2 < l_0^2$  , the orbit is bound between  $r_1 < r < r_2$ . Just for  $l^2 = l_0^2$ , the two bounds coincide and the orbit becomes a circle with an *energy dependent* radius

and angular velocity.

$M = 3$  ,  $a \leq 0$  : For  $l \neq 0$ , the orbit ranges in  $r \geq r_0$ , while for  $l = 0$  it passes through  $r = 0$ .

$M = 2$  ,  $a \leq 0$  : This is the analogue of the  $M = 3$  ,  $a > 0$  case above.

$M = 1$  ,  $a \leq 0$  : This is the analogue of the  $M = 3$  ,  $a \leq 0$  case above, with the difference that when  $a > 0$  the orbit never passes the origin even for  $l = 0$ .

## 4.3 Quantitative features

### 4.3.1 The infinite orbits

As the above description shows, (for both  $\varepsilon = \pm 1$  cases) there are many regimes in which the orbit extends to the infinite region  $r \rightarrow \infty$ . The asymptotic behavior of such orbits is deduced from the study of the asymptotic behaviors of  $U(r)$  and  $\omega(r)$ . For the present purpose, we need only to the limiting values, which according to eqs.(30),(31),(35), are

$$r \rightarrow \infty \quad \begin{cases} U(r) \rightarrow U_0 \\ \omega(r) \rightarrow 0 \end{cases} \quad (37)$$

where  $U_0 = U_0(E)$  is

$$U_0 = \begin{cases} \varepsilon \left( \frac{1}{(E+\eta)^2} - 1 \right) & , \quad M \geq 3 \\ 0 & , \quad M = 1 \end{cases} \quad (38)$$

These limiting values, according to the differential eqs.(24),(25), correspond to straight line asymptotic orbits, in the  $\theta = \theta_0$  planes, with a slope  $dr/dx = \pm\sqrt{U_0}$ . This means that, in all the cases with  $U_0 \geq 0$ , the S-P system asymptotically looks like a pair of *flat*  $(d-1)$ -branes, with a relative rotation (boost) in one direction with an angle  $\gamma$  (a velocity  $v$ ) satisfying

$$U_0 = \begin{cases} \tan^2\gamma & , \quad \varepsilon = +1 \\ v^2 & , \quad \varepsilon = -1 \end{cases} \quad (39)$$

Consequently, the energy-dependences of  $\gamma$  and  $v$  are determined by eq.(38). For  $M = 1$ , this indicates that all values of  $E$  yield to a *parallel static* configuration of the S&P-branes at infinite distances. For  $M \geq 3$ , it gives

$$E + \eta = \begin{cases} |\cos\gamma| & , \quad \varepsilon = +1 \\ 1/\sqrt{1-v^2} & , \quad \varepsilon = -1 \end{cases} \quad (M \geq 3) \quad (40)$$

Accordingly, the allowed values of  $E$  for these infinite orbits range as

$$\begin{cases} -\eta \leq E \leq 1 - \eta & , \quad \varepsilon = +1 \\ E \geq 1 - \eta & , \quad \varepsilon = -1 \end{cases} \quad (M \geq 3) \quad (41)$$

For  $\varepsilon = +1$ , the bound  $E = 1 - \eta$  corresponds to an asymptotic parallel ( $\gamma = 0$ ) or anti-parallel ( $\gamma = \pi$ ) S-P configuration, while  $E = -\eta$  corresponds to an asymptotic orthogonal ( $\gamma = \pi/2$ ) situation. For  $\varepsilon = -1$ , the bound  $E = 1 - \eta$  corresponds to an asymptotic static ( $v = 0$ ) moving configuration, while  $E = +\infty$  corresponds to an asymptotic light-like ( $v = 1$ ) motion. The values of  $E$  near these two extremes correspond to the Newtonian and Relativistic limits respectively.

### 4.3.2 The circular orbits

Among the graphs of Fig.(1), regimes can be distinguished, for which the orbits have a constant radius  $r = R$ . For each specific value of  $E$ , such an orbit (if any) is characterized by the values of  $l^2$  that touch the extremum points of the graph for  $f(r)$ , i.e.

$$f(R) = l_0^2 \quad , \quad f'(R) = 0 \quad (42)$$

Noting to the sign of the ‘effective force’, the maximum (minimum) points of  $f(r)$  characterize the stable (unstable) circular orbits. Among the space-like cases with  $M \geq 2$ , we see that there are no circular orbits. Among the time-like orbits, however, we find a special type of the circular orbits one for each dimension  $M \geq 2$ . These consist of the following cases:

$M \geq 5$  ,  $a < 0$  ; *Unstable circular orbits:*

The radius ( $R$ ), angular momentum ( $l_0$ ), and angular velocity ( $\omega_0$ ) of the orbits, by eqs.(31),(35),(42), are found to be

$$\begin{aligned} R &= \left( \frac{M-4}{2} \frac{Q}{1+2\eta/E} \right)^{\frac{1}{M-2}} \\ l_0^2 &= \frac{M-2}{2} E^2 Q R^{4-M} \\ \omega_0 &= \frac{\left[ \left( \frac{M-2}{M-4} \right) \left( 1 + 2\frac{\eta}{E} \right) \right]^{1/2}}{R \left[ \left( \frac{M-2}{M-4} \right) \left( 1 + 2\frac{\eta}{E} \right) - \frac{\eta}{E} \right]} \end{aligned} \quad (43)$$

It is amazing that the velocity  $v_0 = R\omega_0$  for these orbits turns to be independent of  $Q$ .

$M = 4$  ,  $a = 0$  ; *Marginally stable circular orbits:*

Such orbits, having *arbitrary radiuses*, are special to the dimension  $M = 4$  and occur for very specific values of  $(E, l)$  which yield  $f(r) \equiv l^2$  for all values of  $r$ . So, for such orbits we must have

$$E = -2\eta \quad , \quad l_0^2 = 4Q \quad (44)$$

However, since by the eq.(34) we must have  $E > -\eta$ , such ‘marginally stable’ circular orbits can only happen in the case of a brane-anti-brane system with  $\eta = 1$ , having the energy  $E = 2$ . A circle of radius  $R$  in this case is traversed with the angular velocity

$$\omega_0 = \frac{2\sqrt{Q}}{2Q + R^2} \quad (45)$$

$M = 3$  ,  $a > 0$  ; *Stable circular orbits:*

The formulas for  $R$ ,  $l_0^2$ ,  $\omega_0$  are just given by eqs.(43) with  $M = 3$ . Again the velocity on this circle is independent of  $Q$ .

$M = 2$  ; *Stable circular orbits:*

In this case , the values of  $R, l_0^2, \omega_0$  are

$$\begin{aligned} R &= e^{2\eta/EQ-1/2} \\ l_0^2 &= 1/2E^2QR^2 \\ \omega_0 &= \frac{\sqrt{Q/2}}{R(Q/2 - \eta/E)} \end{aligned} \quad (46)$$

Despite the  $M \geq 5$  or  $M = 3$  cases, the velocity on these circles does depend on  $Q$ . Because of the natural bound  $r \leq 1$  in  $M = 2$ , for these orbits to be realized we must have  $4\eta/EQ < 1$ .

### 4.3.3 The orbits crossing the origin

Amongst the various regimes, distinguishable from Fig.(1), there are cases where the orbit can approach, or pass through, the origin ( $r = 0$ ). Such regimes (orbits) are interesting, since they give descriptions for branes that intersect with, and/or fall on each other. The approach towards the origin may take place at finite or infinite values of  $x$ . In the former case, the two branes intersect or collide (depending on  $\varepsilon = +1$  or  $-1$ ) and pass through each other, while in the latter case they meet (and coincide) only asymptotically. For a quantitative description, we consider space- and time-like orbits separately.

*Space-like case:*

The only space-like orbit passing the origin occurs for  $M = 1$  ,  $a > 0$ . In such a case (having naturally  $l = 0$ ), we obtain a 1-dimensional periodic orbit which, several times with a period  $L$ , intersects the  $x$ -axis and then goes through a maximum at  $r = r_0$ . It is easy to see that in this case  $U(r)$  has the form

$$U(r) = U_0 \frac{1 - r/r_0}{(1 - r/r_1)^2} \quad (47)$$

where  $r_0 := -(2\eta + E)/EQ$ ,  $r_1 := -(\eta + E)/EQ$  ( $r_0 > r_1$ ) and  $U_0$  is defined as in the first row of eq.(38). The period  $L$  of this orbit then is calculated as <sup>6</sup>

$$L = 4 \int_0^{r_0} \frac{dr}{\sqrt{U(r)}} = \frac{8}{3Q} (-\eta E)^{-3/2} [4 - (1 - \eta E)(2 + \eta E)^{1/2}] \quad (48)$$

(note that  $0 < -\eta E < 2$ , by  $a > 0$ ). The periodicity of the orbit along the  $x$ -direction hints that  $x$  may be a compactified coordinate, wrapped along a circle of radius  $L/2\pi$ , in which case the energy (stress) required for such a wrapping of the P-brane around the compact direction of the S-brane is obtained by reversing the eq.(48) for  $E = E(L)$ .

*Time-like case:*

The origin crossing time-like orbits occur in each of the following situations:

- (1)  $M \geq 5$ , arbitrary  $E$  &  $l$
- (2)  $M = 4$ ,  $l^2 \leq l_0^2$ , arbitrary  $E$
- (3)  $M = 3$ ,  $l = 0$ , , arbitrary  $E$
- (4)  $M = 2$ ,  $l = 0$ , , arbitrary  $E$
- (5)  $M = 1$  ( $l = 0$ ),  $a(E) \leq 0$ .

As was pointed above, the orbit may pass through the origin at a finite time in which case its passage takes place several times with a definite period  $T$ ,

$$T = 2 \int_0^{r_0} \frac{dr}{\sqrt{U(r)}}, \quad (49)$$

or it may tend to the origin during an infinite ‘fall time’ which is the characteristic of a ‘black’ singularity at  $r = 0$  [6]. Generally, the criterion for finite (infinite)-ness of the fall time is that the contribution to the above integral from the region  $r \rightarrow 0$ ,

$$\Delta T(r) := \int_{r \rightarrow 0} \frac{dr}{\sqrt{U(r)}}, \quad (50)$$

vanishes (diverges). For each of the above cases, one can see that

$$\begin{array}{lll} M \geq 5 & : & \Delta T(r) \sim 1/r^{(M-4)/2} \quad , \quad \omega(r) \sim \omega_0 r^{M-4} \\ M = 4 \quad (l^2 < l_0^2) & : & \Delta T(r) \sim -\ln r \quad , \quad \omega(r) \sim \omega_0 \\ M = 4 \quad (l^2 = l_0^2) & : & \Delta T(r) \sim 1/r \quad , \quad \omega(r) \sim \omega_0 \\ M = 3 \quad (l = 0) & : & \Delta T(r) \sim r^{1/2} \quad , \quad \omega(r) \equiv 0 \\ M = 2 \quad (l = 0) & : & \Delta T(r) \sim \int \frac{dr}{\sqrt{-\ln r}} \quad , \quad \omega(r) \equiv 0 \\ M = 1 \quad (l = 0) & : & \Delta T(r) \sim r \quad , \quad \omega(r) \equiv 0 \end{array} \quad (51)$$

---

<sup>6</sup>The factor 4 in eq.(48) is related to the fact that the section curve of the the P-brane  $Y^1 = Y^1(x)$  can not involve a sharp turning point at  $Y^1 = 0$ , but it contains two symmetric semi-cycles with their turning points at  $Y^1 = \pm r_0$ , since otherwise a  $\delta$ -force at  $r = 0$  would be required.

where  $l_0^2 := E^2 Q$ ,  $\omega_0 := l/EQ$ . We have appended to this list a third column for angular velocities near  $r = 0$ , so as to clarify the status of the angular motion in this vicinity. From this list it is evident that all of the  $M \geq 4$  orbits have infinite fall times ( $\Delta T \rightarrow \infty$ ). However, while all  $M \geq 5$  orbits tend *linearly* (as  $\omega \rightarrow 0$ ) towards the origin, the  $M = 4$  orbits approach *spirally* to that point (as  $\omega \rightarrow \omega_0$ ). On the other hand, all  $M \leq 3$  orbits tending to the origin have a finite fall time ( $\Delta T \rightarrow 0$ ), and the corresponding motions are in the form of periodic 1-dimensional oscillations around the origin (as  $\omega \equiv 0$ ).

## 5 The S-P system with $d_s > d_p$

Here the second row of (9) defines  $(x^a, y^A)$ . The Lagrangian describing the mono-dimensional solutions:  $Y^i = Y^i(x)$ ,  $Y^m = Y^m(x)$ , with  $x$  being one of the  $x^a$ 's, turns to be

$$L = -H^{-m/2}[1 + \varepsilon(\dot{Y}^i)^2 + \varepsilon H(\dot{Y}^m)^2]^{1/2} \quad (52)$$

where the exponent  $m$  is a function of dimensions as

$$m := 2\alpha(d_s)\alpha(d_p) + \tilde{d}_s d_p / \bar{D} \quad (53)$$

with  $\alpha(d)$  defined in eq.(3). Note that in eq.(52),  $H$  is a function only of  $Y^m$ 's through their modulus. As eq.(53) shows,  $m$  is a generally non-integer real number. However, according to the 'intersection rule' of the 'marginal' brane intersections [4, 16], a pair of  $(d_s - 1, d_p - 1)$ -branes (not necessarily a S-P configuration) sharing in a number  $(\delta - 1)$  of their worldvolume directions constitutes a marginally stable configuration provided

$$\delta = -2\alpha(d_s)\alpha(d_p) + d_s d_p / \bar{D} \quad (54)$$

Combining eqs.(53),(54), one obtains

$$m = d_p - \delta \quad (55)$$

showing that in such occasions  $m$  is a positive integer specifying the number of the (rotation) angles between the two branes, when they are 'flattened' in all of their worldvolume directions [4]. For an arbitrary situation, however one can see, using the relations of the type of eq.(3), that  $m$  satisfies

$$-2 \leq m \leq 2 \quad (56)$$

For a marginal intersection, thus the only possibilities are  $m = 0, 1, 2$ .

The conserved quantities (charges) corresponding to the symmetries (6)-(8) consist of

$$E := \dot{Y}^i \frac{\partial L}{\partial \dot{Y}^i} + \dot{Y}^m \frac{\partial L}{\partial \dot{Y}^m} - L = \frac{H^{-m/2}}{\sqrt{1 + \varepsilon(\dot{Y}^i)^2 + \varepsilon H(\dot{Y}^m)^2}} \quad (57)$$

$$J^{mn} := Y^m \frac{\partial L}{\partial \dot{Y}^n} - Y^n \frac{\partial L}{\partial \dot{Y}^m} = -\varepsilon \frac{H^{-m/2+1}(Y^m \dot{Y}^n - Y^n \dot{Y}^m)}{\sqrt{1 + \varepsilon(\dot{Y}^i)^2 + \varepsilon H(\dot{Y}^m)^2}} \quad (58)$$

$$P^i := \frac{\partial L}{\partial \dot{Y}^i} = -\varepsilon E \dot{Y}^i \quad (59)$$

$$J^{ij} := Y^i \frac{\partial L}{\partial \dot{Y}^j} - Y^j \frac{\partial L}{\partial \dot{Y}^i} = P^i Y^j - P^j Y^i \quad (60)$$

By eqs.(57),(59) the ‘velocity’ components in the  $y^i$ -directions are conserved quantities. Owing to the Lorenz invariance of the action (52) along the  $(x, y^i)$  directions, one can rotate these coordinates so as to obtain  $\dot{Y}^i = 0$ . In such a Lorenz frame,  $Y^i$ 's become constant coordinates, which can be taken to be zero, and hence by eqs.(59),(60) one obtains  $P^i = J^{ij} = 0$ . Accordingly, the orbit  $Y^m = Y^m(x)$ ,  $Y^i(x) = 0$  is described by means of the two conservation laws (57),(58) now with  $\dot{Y}^i = 0$ . Just as in the case with  $d_s = d_p$ , one can see that the orbit lies in a 2D plane spanned within the  $y^m$ -directions. Choosing the polar coordinates  $(r, \theta)$  on this plane, in analogy to eqs.(22),(23), one obtains

$$\frac{H^{-m/2}}{\sqrt{1 + \varepsilon H(r)(\dot{r}^2 + r^2 \dot{\theta}^2)}} = E \quad (61)$$

$$\frac{H^{-m/2+1}(r)r^2 \dot{\theta}}{\sqrt{1 + \varepsilon H(r)(\dot{r}^2 + r^2 \dot{\theta}^2)}} = l \quad (62)$$

where  $r^2 := Y^m Y^m$ . In analogy to eqs.(24),(25), these two equations give

$$\dot{r}^2 = U(r) := \frac{f(r) - l^2}{E^2 r^2 H^2(r)} \quad (63)$$

$$\dot{\theta} = \omega(r) := \frac{l}{E r^2 H(r)} \quad (64)$$

Here  $f(r)$  has the following definition

$$f(r) := \varepsilon r^2 H(r) [H^{-m}(r) - E^2] \quad (65)$$

It is convenient to re-express  $f(r)$  as a function of  $H$  as

$$f(H) = \begin{cases} \varepsilon Q^n \frac{H(H^{-m} - E^2)}{(H-1)^n} & , \quad M \neq 2 \\ \varepsilon e^{-2H/Q} H(H^{-m} - E^2) & , \quad M = 2 \end{cases} \quad (66)$$

where  $n := 2/(M-2)$ . Again the solutions for  $(r(x), \theta(x))$  are found by integrations as in eqs.(26),(27) and the solution for  $r(\theta)$  is found directly from eq.(28). Also, as eqs.(63),(64) indicate, the orbital ‘motion’ is composed of a *monotonic* angular ‘motion’ around  $r = 0$  and a radial ‘motion’ within a range specified by the inequality (32). Accordingly, the qualitative description of the orbits, as in the past, proceeds via the study of the  $f(r)$  diagrams sketched in Figs.(2)-(6). By eq.(65), a marginal configuration of two parallel branes in this case corresponds to the values  $m = 0$ ,  $E = 1$ ,  $l = 0$ .



## 5.1 An overall look on the orbits

A large variety of the regimes and phases of the effective radial motion are revealed, when one travels through several transverse dimensions and changes the (the ranges of) the three parameters  $(m, E^2, l^2)$ . The corresponding diagrams for the function  $f(r)$  are shown in Figs.(2)-(6) for the case of the space-like orbits; the time-like case is covered by reversing the same diagrams. As in the previous  $(d_s = d_p)$  case, all the dimensions  $M \geq 5$  with fixed  $(m, E)$  share a common qualitative behavior. Different behaviors appear for  $M \leq 4$ . Some more or less novel features in this case are the appearance of the bound, circular (stable/unstable), origin-crossing and infinite orbits as well as the co-existing phases of the bound and infinite orbits in the dimensions  $M \geq 1$  and in both the space- and time-like cases. A completely new behavior occurs for the case of the space-like orbits in dimension  $M = 3$ , where  $f(r)$  possesses a pair of local minimum and maximum points. In such a case (for suitable values of  $l^2$ ) a regime with co-existing phases of an origin-crossing and a bound oscillatory orbits is realized. Marginally stable circular orbits, like the previous case, occur just for a particular time-like case in  $M = 4$ .

## 5.2 Some quantitative features

### 5.2.1 The infinite orbits

The cases with infinitely extended orbits correspond to those values of  $(M, m, l, E, \varepsilon)$  that the solution to the inequality  $U(r) \geq 0$  includes the  $r \rightarrow \infty$  region. A variety of these orbits (for all  $M \neq 2$ ) are distinguishable among the Figs.(2)-(6). It is easy to check, as in the  $d_s = d_p$  case, that all such orbits also in this case exhibit a straight line-like asymptotic behavior which is governed by the eqs.(37), where the parameter  $U_0$  is

$$U_0 = \begin{cases} \varepsilon(1 - E^2)/E^2 & , \quad M \geq 3 \\ \infty & , \quad M = 1, m < -1 \\ 1/E^2 & , \quad M = 1, m = -1 \\ 0 & , \quad M = 1, m > -1 \end{cases} \quad (67)$$

The allowed cases are those with  $U_0 \geq 0$ . So, using eq.(39), one obtains

$$E = \begin{cases} |\cos\gamma| & , \quad \varepsilon = +1 \\ 1/\sqrt{1 - v^2} & , \quad \varepsilon = -1 \end{cases} \quad (M \geq 3) \quad (68)$$

Thus, for such orbits, in the space-like case we have  $0 \leq E \leq 1$ , while in the time-like case  $E \geq 1$ . In the former case the  $E = 0$  ( $E = 1$ ) bound corresponds to an asymptotic orthogonal (parallel) configuration, while in the latter the  $E = 1$  ( $E = \infty$ ) bound corresponds to an asymptotic static (light-like) motion. Again, the dimension

$M = 1$  exhibits an exceptional behavior: for  $m < -1$  ( $m > -1$ ) the (S,P)-branes are asymptotically perpendicular (parallel) to each other, while for  $m = -1$  they make an asymptotic angle  $\gamma = \tan^{-1}(1/E)$ .

The  $E \rightarrow 0$  limit in the space-like case is particularly interesting because it corresponds to a generalized *marginal* configuration of two branes in which one of the branes is curved. Such a configuration may preserve some fraction of SUSY at least in some special cases. By eqs.(63),(64), one sees that  $U, \omega \rightarrow \infty$  when  $E \rightarrow 0$ , showing that the P-brane in this limit is totally projected into a *planar* curve lying in the transverse space of the S-brane and so the two branes are ‘orthogonal’ to each other. One can show that the orbit’s equation (eq.(28)) in the special case with  $m = 1$  and in the limit  $E \rightarrow 0$  has the solution:  $r = l/\cos\theta$  corresponding to an straight line of separation  $r_0 = l$  relative to the source at  $r = 0$ . This corresponds to the marginal configuration of two different branes at one *right* angle preserving a 1/4 SUSY fraction, which is a special case of the solutions found in [16, 4].

### 5.2.2 The circular orbits

Despite the  $d_s = d_p$  case, here circular orbits of both the space- and time-like natures are allowable for all  $M \geq 2$ . Several such orbits are distinguished by the extremum points of the graphs in Figs.(2)-(6) and are classified in the Table (1) below. The symbols  $s, u$  and  $ms$  in this table refer to the stable, unstable and marginally stable orbits respectively.

	$M = 2$	$M = 3$	$M = 4$	$M \geq 5$
$m < -1$	$\varepsilon = \pm 1(s)$	$\varepsilon = +1(s, u)$	$\varepsilon = +1(u)$	$\varepsilon = +1(u)$
$m = -1$	"	$\varepsilon = +1(s)$	"	"
$-1 < m < 0$	"	"	"	"
$m = 0$	"	–	–	$\varepsilon = \pm 1(u)$
$0 < m < 1$	"	$\varepsilon = -1(s)$	$\varepsilon = -1(u)$	$\varepsilon = -1(u)$
$m = 1$	$\varepsilon = -1(s)$	"	$\varepsilon = -1(ms)$	"
$m > 1$	"	"	$\varepsilon = -1(s)$	"

Table (1): circular orbits for  $d_s > d_p$

Each orbit in Table (1) occurs only for a specific range of  $E$  and a suitable value of  $l$ . The radius  $R$  of a circular orbit of energy  $E$  is determined, through its corresponding value of  $H$ , by the equation

$$\begin{aligned}
 (1 - m - n)H^{1-m} - (1 - m)H^{-m} + E^2(n - 1)H + E^2 &= 0 \quad , \quad M \neq 2 \\
 \left(\frac{2H}{Q}\right)^{1-m} - (1 - m)\left(\frac{2H}{Q}\right)^{-m} - E^2\left(\frac{Q}{2}\right)^m\left(\frac{2H}{Q} - 1\right) &= 0 \quad , \quad M = 2 \quad (69)
 \end{aligned}$$

Two distinguished behaviors occur in  $M = 3, 4$  cases. For  $M = 3$ ,  $m < -1$ , and at  $E = E_m$ ,  $H = H_m$  with

$$\begin{aligned} H_m &= \sqrt{\frac{m-1}{m+1}} \\ E_m^2 &= \left(\frac{m-1}{m+1}\right)^{-(m+1)/2} (m-1)(m+\sqrt{m^2-1}) \end{aligned} \quad (70)$$

the first and second derivatives of  $f(H)$  simultaneously vanish and a ‘semi-stable’ (space-like) circular orbit of radius  $R = Q/(H_m - 1)$  is obtained. In the range of energy  $1 < E < E_m$ , this orbit splits into a pair of stable and unstable circles at different radii at the same value of  $E$  but different values of  $l^2$ . For  $M = 4$ ,  $m = 1$ , and at values  $E = 1$ ,  $l^2 = Q$ , a marginally stable (time-like) circular orbit of arbitrary radius is realized. For the same value of  $E$  but with  $l^2 < Q$ , this circle is deformed into a ‘spiral curve’ of the form

$$r(\theta) = Re^{\nu\theta} \quad (71)$$

where  $\nu := \sqrt{Q - l^2}/l$  and  $R$  is any arbitrary initial radius.

### 5.2.3 The coincident (S,P) configurations

In addition to the above mentioned finite size circular orbits, there exist other limiting cases which are characterized by circles of zero radius with a vanishing, finite or infinite angular velocity. In a time-(space-)like situation, such a solution describes a coincident (S,P) configuration in which the P-brane, in some cases, has a non-vanishing spin (torsion) equal to  $\omega(r \rightarrow 0)$ . Such orbits, which are the  $r = 0$  solutions to the equations of motion, are specified by those values of the parameters satisfying

$$U(r \rightarrow 0) = 0 \quad , \quad U'(r \rightarrow 0) = 0 \quad (72)$$

The solution is stable (unstable) provided  $U''(r \rightarrow 0)$  to be negative (positive). The expansion of  $U(r)$  near  $r = 0$  up to a few leading terms for different values of  $(M, m)$ , thus gives rise to a classification of the coincident (S,P) solutions as is indicated in Table (2) below.

$M = 3$ ( $\omega = \infty$ )	$M = 4$ ( $\omega = \omega_0$ )	$M \geq 5$ ( $\omega = 0$ )
$m = -1$ $\varepsilon = +1(s)$	$-\frac{1}{2} < m < 0$ $\varepsilon = -1(s), +1(u)$	$\frac{3-M}{M-2} < m < 0$ $\varepsilon = -1(s), +1(u)$
—	$m = 0$ $\varepsilon = \pm 1(s, u)$	$m = 0$ $\varepsilon = \pm 1(s, u)$
—	$0 < m < 1$ $\varepsilon = \pm 1(s)$	$m > 0$ $\varepsilon = +1(s), -1(u)$
—	$m \geq 1$ $\varepsilon = \pm 1(s), -1(u)$	—

Table (2): coincident (S,P) solutions for  $d_s > d_p$

As in Table (1), each of the solutions in Table (2) is achieved for a suitable range or fixed values of  $(E, l)$ . As the first row in this table shows, while the  $M = 4$  solutions carry a finite spin or torsion ( $\omega = \omega_0 := l/EQ$ ), all the  $M \geq 5$  solutions are without spin and torsion ( $\omega = 0$ ). On the other hand the  $M = 3$  solution has an infinite torsion ( $\omega = \infty$ ) which means that one of the P-brane directions is crumpled (i.e., wrapped on a circle of vanishing radius) around the S-brane directions.

#### 5.2.4 The origin-crossing orbits

Orbits of this type occur in cases where the solution to the inequality  $U(r) \geq 0$  involves the  $r = 0$  point. Generically, such an orbit is bounded between  $r = 0$  and  $r = r_0$ , where  $U(r_0) = 0$  (through in some cases  $r_0 \rightarrow \infty$ ). The origin may be crossed or approached by the orbit depending on that the quantity defined in eq.(50) (which is denoted by  $\Delta X$  below to include both the space- and time-like cases) vanishes or diverges respectively. The various origin crossing orbits of both characters, for different values of  $(M, m)$ , are classified in Table (3) below.

$(\varepsilon, \Delta X)$	$M = 1$	$M = 2$	$M = 3$	$M = 4$	$M \geq 5$
$m < 0$	$(\pm 1, 0)$	$(+1, 0)$	$(+1, 0)$	$(+1, 0)$	$(+1, 0)$ , $m < \frac{4-M}{M-2}$ $(+1, \infty)$ , $m \geq \frac{4-M}{M-2}$
$m = 0$	"	$(\pm 1, 0)$	$(\pm 1, 0)$	$(\pm 1, \infty)$	$(\pm 1, \infty)$
$m > 0$	"	$(-1, 0)$	$(-1, 0)$	$(-1, \infty)$	$(-1, \infty)$

Table (3): origin-crossing orbits for  $d_s > d_p$

## 6 The S-P system with $d_s < d_p$

By defining  $(x^a, y^A)$  as in the third row of (9), the Lagrangian  $\mathcal{L}$  describing the embedding coordinates  $Y^A = Y^A(x^\mu, y^i)$  is found to be

$$\mathcal{L} = -H^{-m/2} \det^{1/2}(\delta_\nu^\mu + H \partial^\mu Y^A \partial_\nu Y^A) \det^{1/2}(\delta_{ij} + \partial_i Y^A \partial_j Y^A) \quad (73)$$

where  $m$  is defined as in eq.(53) with  $(d_s, d_p)$  interchanged, i.e.

$$m := 2\alpha(d_s)\alpha(d_p) + d_s \tilde{d}_p / \bar{D} \quad (74)$$

When the ‘marginality’ condition (54) is satisfied, in analogy to eq.(55),  $m$  coincides to the number of the non-zero angles for marginal intersection:

$$m = d_s - \delta \quad (75)$$

A major difference between this ( $d_s < d_p$ ) case and the previous ( $d_s \geq d_p$ ) ones is that the Lagrangian (73), unlike (13),(52), contains explicit dependences on (the subset  $y^i$  of) the parameterization coordinates  $(x^\mu, y^i)$  themselves, through the dependence of  $H$  on

$$r = \sqrt{(y^i)^2 + (y^A)^2} \quad (76)$$

This property (generally) prevents the possibility of existing any mono-dimensional solution, which as in the previous cases depends only on one of the coordinates  $(x^\mu, y^i)$ . In particular, parallel relatively moving configurations in this case are not allowable (this is unlike to the situation where the roles of  $d_s$  and  $d_p$  are interchanged !). However, other interesting possibilities for solutions of the Lagrangian (73) exist which are explained below.

*(Semi-)cylindrical configurations:*

Interesting configurations occur when a number  $\delta$  of the *flat* S-brane directions are parallel, and the rest  $(d_s - \delta)$  of them are perpendicular, to a (generally) *curved* P-brane. This means that (for each  $A$ ) a number  $\delta$  of the slopes  $\partial_\mu Y^A$  are vanishing, while the rest  $(d_s - \delta)$  of them tend to infinity <sup>7</sup>. Putting these values in eq.(73), one peaks up a factor  $H^{(d_s - \delta)/2}$  multiplied by a constant infinite factor. Thus, ignoring the irrelevant infinity, the dynamics of the coordinates  $Y^A = Y^A(y^i)$  in this case is governed by

$$\mathcal{L}^* = -H^{(d_s - \delta - m)/2} \det^{1/2}(\delta_{ij} + \partial_i Y^A \partial_j Y^A) \quad (77)$$

The case of a *totally cylindrical* configuration happens when all of the S-brane directions are common to the P-brane, and is covered by the above Lagrangian for  $\delta = d_s$ .

---

<sup>7</sup>More precisely, the slopes for perpendicular  $x^\mu$ 's are in the form of  $\delta$ -functions at the corresponding values of these coordinates.

*Curved marginal intersections:*

An interesting subclass of the above semi-cylindrical solutions consist of the marginal intersections in which one of the two branes (the P-brane) is not necessarily flat. To see that such solutions exist, imagine a pair of branes which are capable of forming a flat marginal solution; that is they obey the rule (54). Assuming a semi-cylindrical configuration with  $\delta$  cylindrical directions, thus the Lagrangian  $\mathcal{L}^*$  becomes

$$\mathcal{L}^* = -\det^{1/2}(\delta_{ij} + \partial_i Y^A \partial_j Y^A) \quad (78)$$

which, unlike eq.(77), does not contain any trace of the spacetime curvature via dependence on  $H$ . The classical solutions for this Lagrangian do represent  $(d_p - d_s)$ -dimensional *minimal* (hyper)surfaces in a  $(\tilde{d}_s + 2)$ -dimensional Euclidean space parametrized by  $(y^i, y^A)$ . These surfaces are solutions to the Laplace equation in the curved space,

$$\square_g Y^A = 0 \quad (79)$$

where  $\square_g := \frac{1}{\sqrt{g}} \partial_i \sqrt{g} g^{ij} \partial_j$  and  $g_{ij}[Y] := \delta_{ij} + \partial_i Y^A \partial_j Y^A$  is the pull-back of the Euclidean  $(\tilde{d}_s + 2)$ -dimensional metric on the minimal surface. For asymptotic flat boundary conditions, the only solutions to this equation are flat surfaces identifying ordinary (flat) orthogonally intersecting S-P systems. For non-asymptotic flat surfaces or surfaces with non-planar boundaries, however, the above equation have non-trivial solutions leading to the curved marginal intersections. In this manner, given every such minimal surface, we can construct a solution of the original theory (73) simply by a cylindrical extension of the minimal surface in some of the S-brane directions.

## 7 Conclusion

In this paper, we have considered the ‘mono-dimensional’ worldvolume solutions for one of a pair of interacting branes in both the space- and time-like configurations, when the other brane is kept fixed and flat (called as the P and S-branes, respectively). For such solutions, the S-brane, which itself has a flat worldvolume geometry, causes the worldvolume of the P-brane to be curved only in one of its (space- or time-like) directions. It was observed that such a configuration is allowed *only* in cases where  $d_s \geq d_p$ . This, for example, implies that when  $d_s < d_p$ , parallel (S,P) configurations in relative transverse motion can not be stable and the motion imposes a curvature on (at least) one of the directions of the P-brane. In all the allowed cases, however, it was shown that the P-brane worldvolume solutions of this type can be described in terms of a set of planar orbits in the subspace transverse to the S-brane, which are parametrized by their ‘energy’ ( $E$ ) and ‘angular momentum’ ( $l$ ) variables. These two parameters fix the form of the solution up to any arbitrary rotation

(translation) along the transverse (parallel) directions of the S-brane. These orbits possess different phases, for different ranges of the parameters  $(E, l)$ , corresponding to phases of an effective 2D motion. These phases are qualitatively described in terms of a set of phase diagrams, corresponding to different values of  $(E, l)$ , or equivalently by the intersections of the graph of an  $E$ -dependent function  $f(r)$  and a line of the constant height  $l^2$ . The ‘effective potential’  $-\frac{1}{2}U(r)$  between (S,P) and their relative ‘angular velocity’  $\omega(r)$  as a function of the transverse distance  $r$  are closely related to this function. Though this function has different expressions in the cases with ‘similar’ and ‘non-similar’ branes, its dependence on  $(d_s, d_p, D)$  always appear through the combinations  $(M, m)$  as

$$\begin{aligned} M &= \tilde{d}_s + 2 \\ m &= 2\alpha(d_s)\alpha(d_p) + \tilde{d}_s d_p / (D - 2) \end{aligned} \tag{80}$$

One of the features that the above analysis reveals is that all  $M \geq 5$  cases, for the same values of  $(E, l)$ , share common qualitative behaviors, while different behaviors appear in  $M \leq 4$  cases. These diagrams also reveal several phases of the ‘effective motion’ such as: the bounded (oscillatory), unbounded (asymptotic free) and circular (rotating) regimes for the space- as well as the time-like configurations. It should be remarked that, although in the previous sections we have considered the cases with  $d_s = d_p$  and  $d_s > d_p$  as representing the configurations with two ‘similar’ and ‘non-similar’ branes, one can fit also some other cases of a two brane system in the same analysis. For example, in 10D supergravity, either of the two configurations of (NS1,D1) and (NS5,NS1) branes can be analyzed as in the  $d_s \neq d_p$  category (section 5). The reason, as can be checked, is that in both these cases the the form-field interaction of the two branes (the WZ term in eq.(5)) has a vanishing contribution to their effective action. Also it should be recognized that the analysis in this paper ignores the effects of the internal gauge fields as well as the external  $B$ -field on the dynamics of p-branes and treats all types of branes as obeying similar dynamics. A possible extension of this work thus may be obtained by inclusion of the above fields in the branes dynamics similar to the one which has been done recently in [17] to handle a  $(D3, D5)$  -branes as a (S,P) system in another geometry. As we have mentioned in the introduction, looking for the exact form of the the p-branes in a multi-angle asymptotic flat intersection has been the main motivation for writing this paper. Nevertheless, the solutions we have considered here are not suitable for describing the configurations with more than one angle. Further, the one-angle asymptotic flat solutions in sections 4,5 are not of the type of the *marginal* intersections with several angles introduced in [10, 11]. For looking for  $m$ -angle configurations, in general, one has to seek for the worldvolume solutions of the P-brane which depend on  $m$  of the directions of the S-brane. Accordingly, one has to solve a set of second order PDE’s in  $m$  dimensions which unlike the 1-dimensional case can not be integrated using its conservation equations. A

perturbative approach in [7], however, shows that solutions of the marginal type for these configurations can be found, provided that the ‘marginality’ property is appropriately defined at infinitely long distances.

## Acknowledgements

The author would like to thank H. Arfaei for his constant encouragements during the course of this work and careful reading of the preprint.

## References

- [1] K.S. Stelle, *Lectures on Supergravity p-branes*, hep-th/9701088
- [2] J. P. Gauntlett, *Intersecting Branes*, hep-th/9705011
- [3] A. A. Tseytlin, *Composite BPS Configurations of p-branes in 10 and 11 dimensions*, hep-th/9702163
- [4] R. Abbaspur, H. Arfaei, *Distributed Systems of Intersecting Branes at Arbitrary Angles*, Nucl. Phys. **B541** (1999) 386-440 (hep-th/9803162)
- [5] M. J. Duff and J. X. Lu, *Black and Super p-branes in Diverse Dimensions* Nucl. Phys. **B416** (1994) 301
- [6] M. J. Duff, R. R. Khuri and J. X. Lu, *String Solitons*, Phys. Rep. **259** (1995) 213
- [7] R. Abbaspur, *Branes at Angles from DBI Action*, hep-th/9903108
- [8] M. Berkooz, M.R. Douglas and R.G. Leigh, *Branes Intersecting at Angles*, Nucl. Phys. **B480** (1996) 265
- [9] J. C. Breckendridge, G. Michaud and R. C. Myers, *New Angles on D-branes*, hep-th/9703041
- [10] M. M. Sheikh Jabbari, *Classification of Different Branes at Angles*, hep-th/9710121
- [11] N. Ohta, P.K. Townsend, *Supersymmetry of M-Branes at Angles*, hep-th/9710129
- [12] R. Abbaspur, in preparation
- [13] A. A. Tseytlin, *No force Condition and BPS Combinations of p-branes in 11 and 10 Dimensions*, hep-th/9609212



- [14] M. Cederwall, *Aspects of D-Brane Actions* hep-th/9612153
- [15] P. Ramond, *Field Theory a Modern Primer*, 1989, The Benjamin/Cummings Publishing Company, Inc.
- [16] R. Argurio, F. Englert, L. Huart, *Intersection Rules for p-branes*, hep-th/9701042
- [17] C.G. Callan, A. Guijosa, K.G. Savvidy, *Baryons and String Creation from the Five-brane Worldvolume Action*, hep-th/9810092

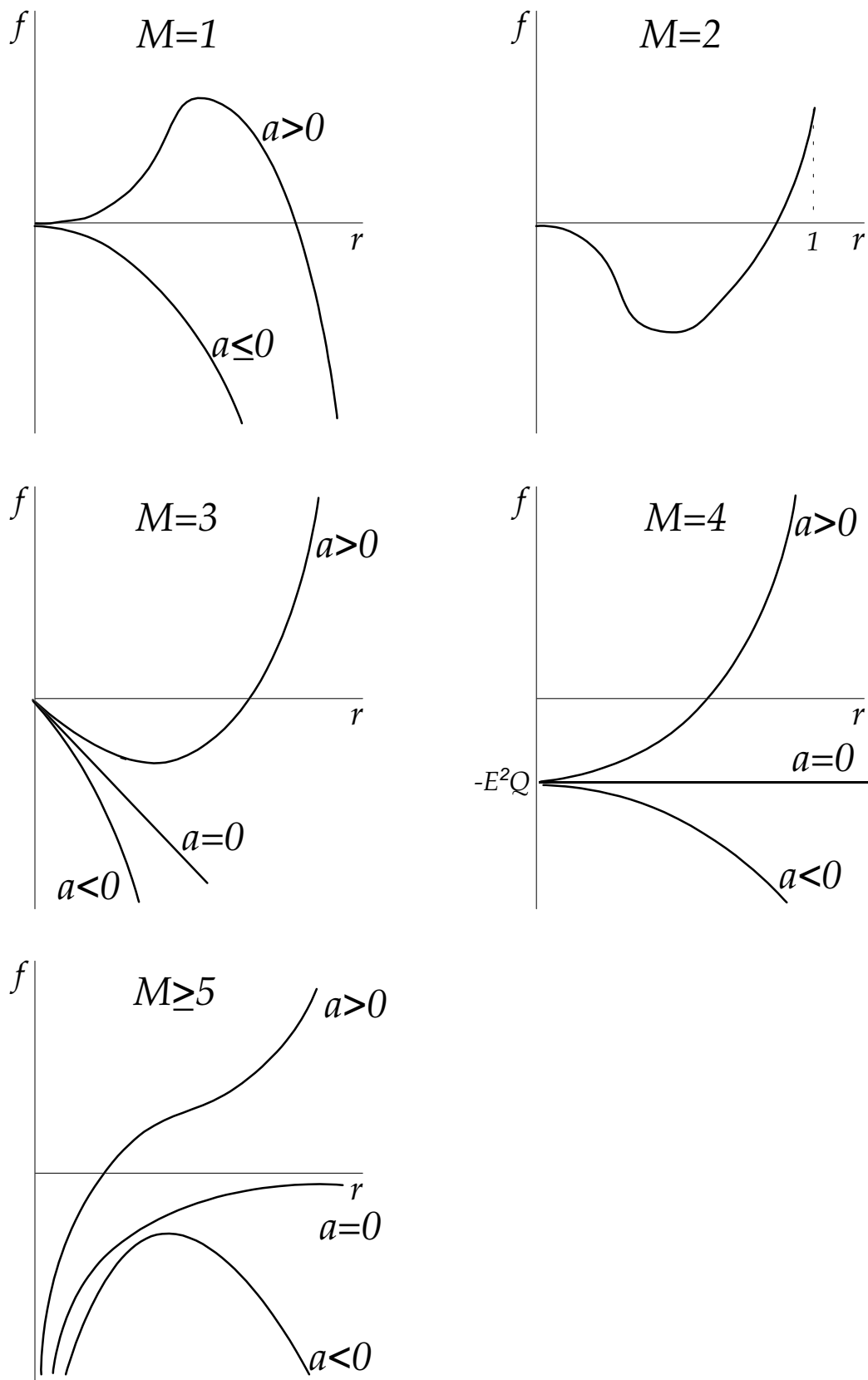
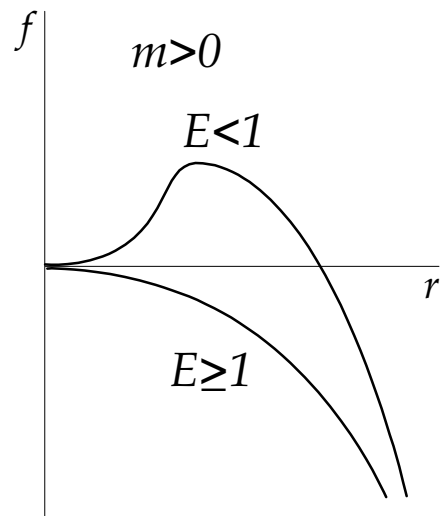
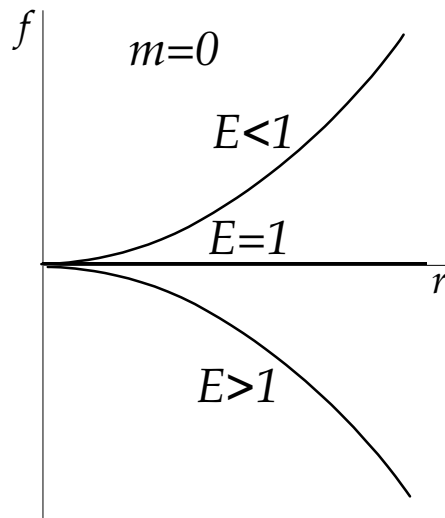
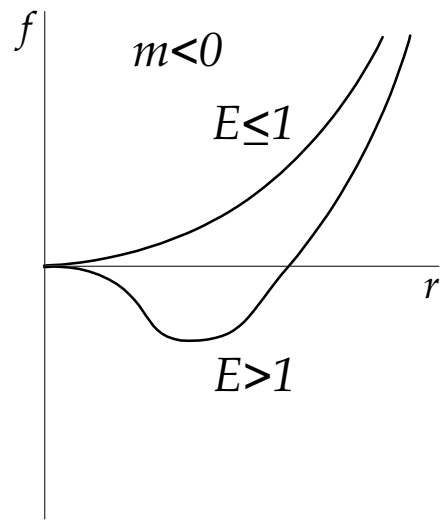


Fig. 1

# $M=1$



**Fig.2**

# $M=2$

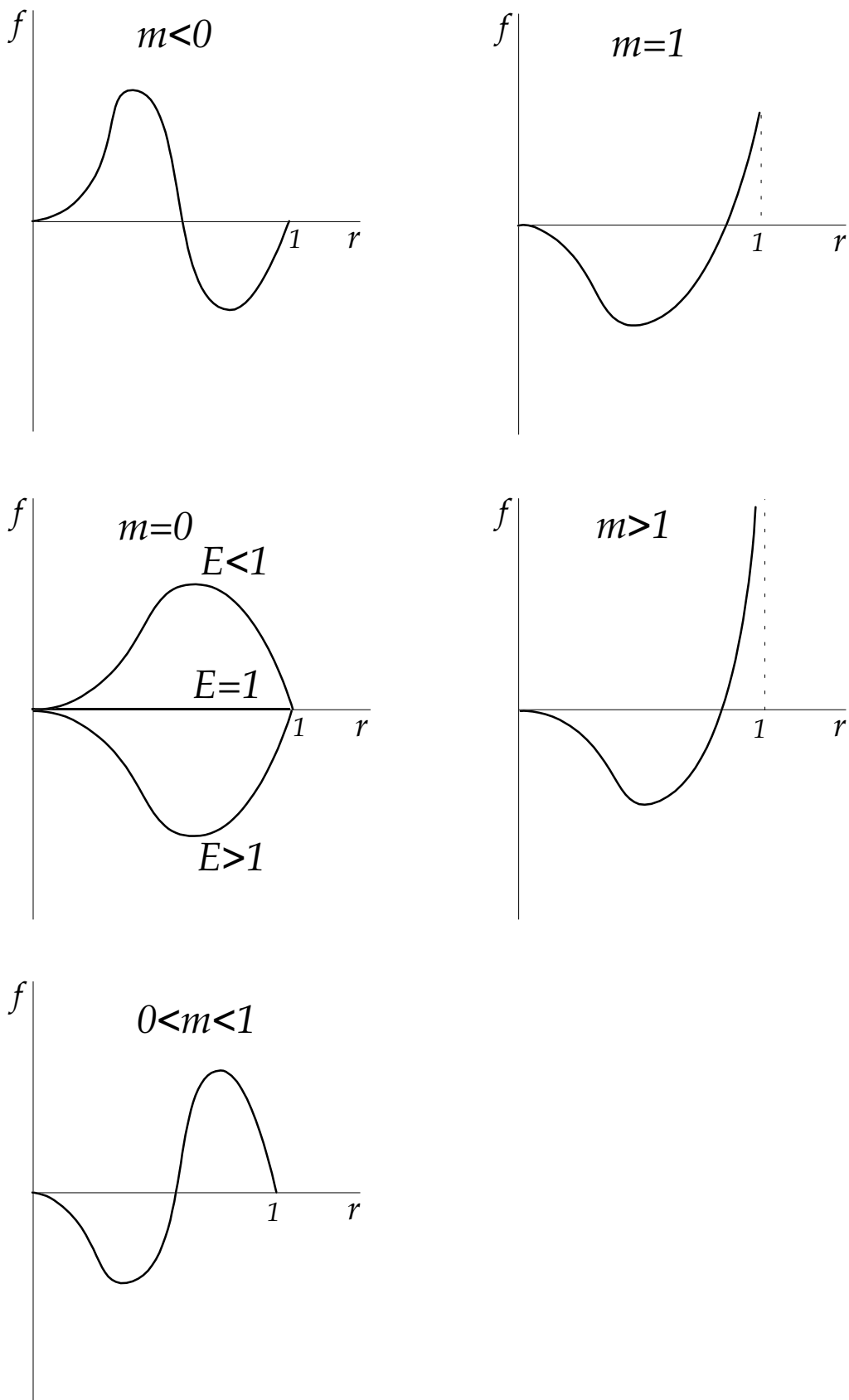


**Fig.3**

# $M=3$

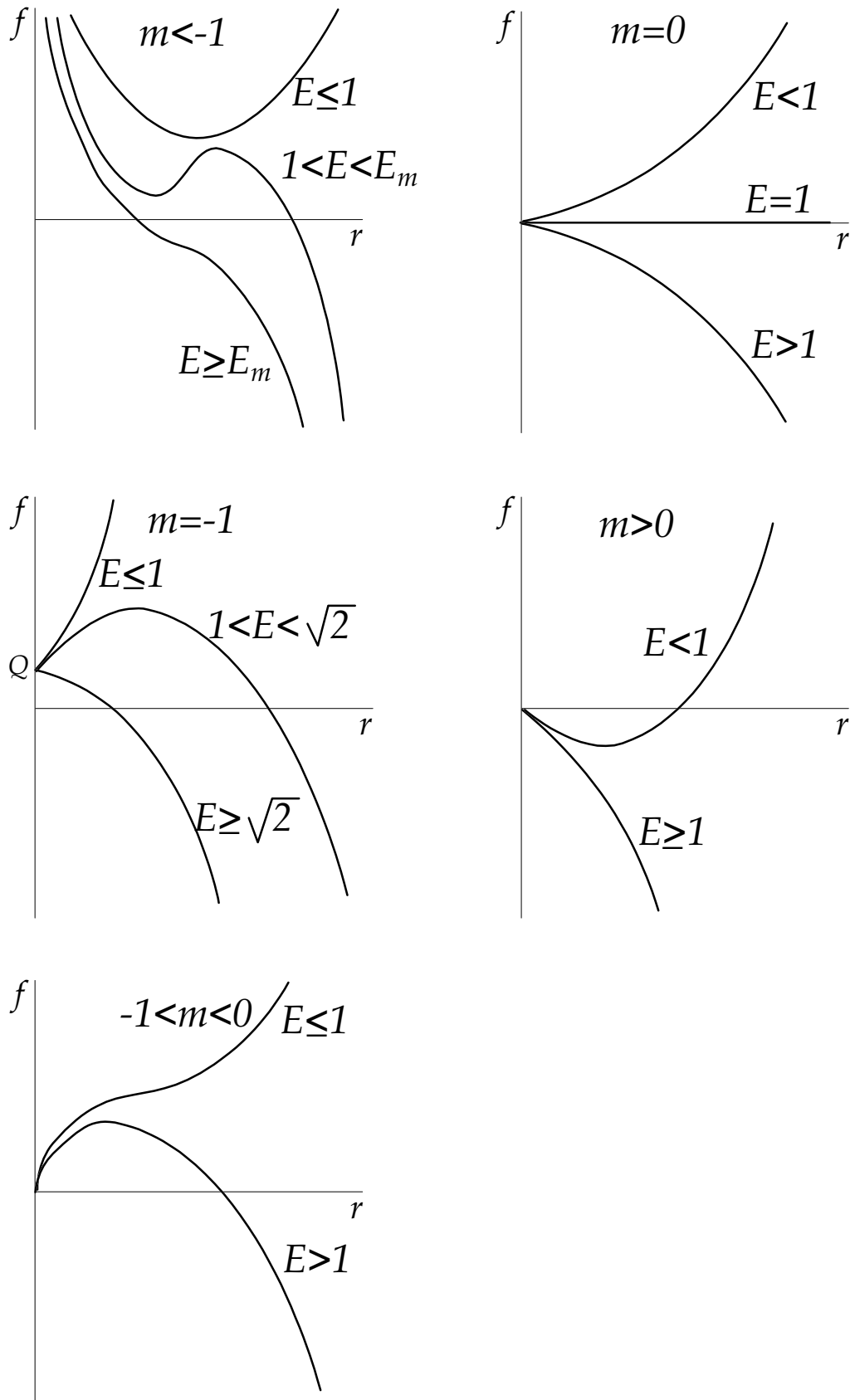


**Fig.4**

# $M=4$

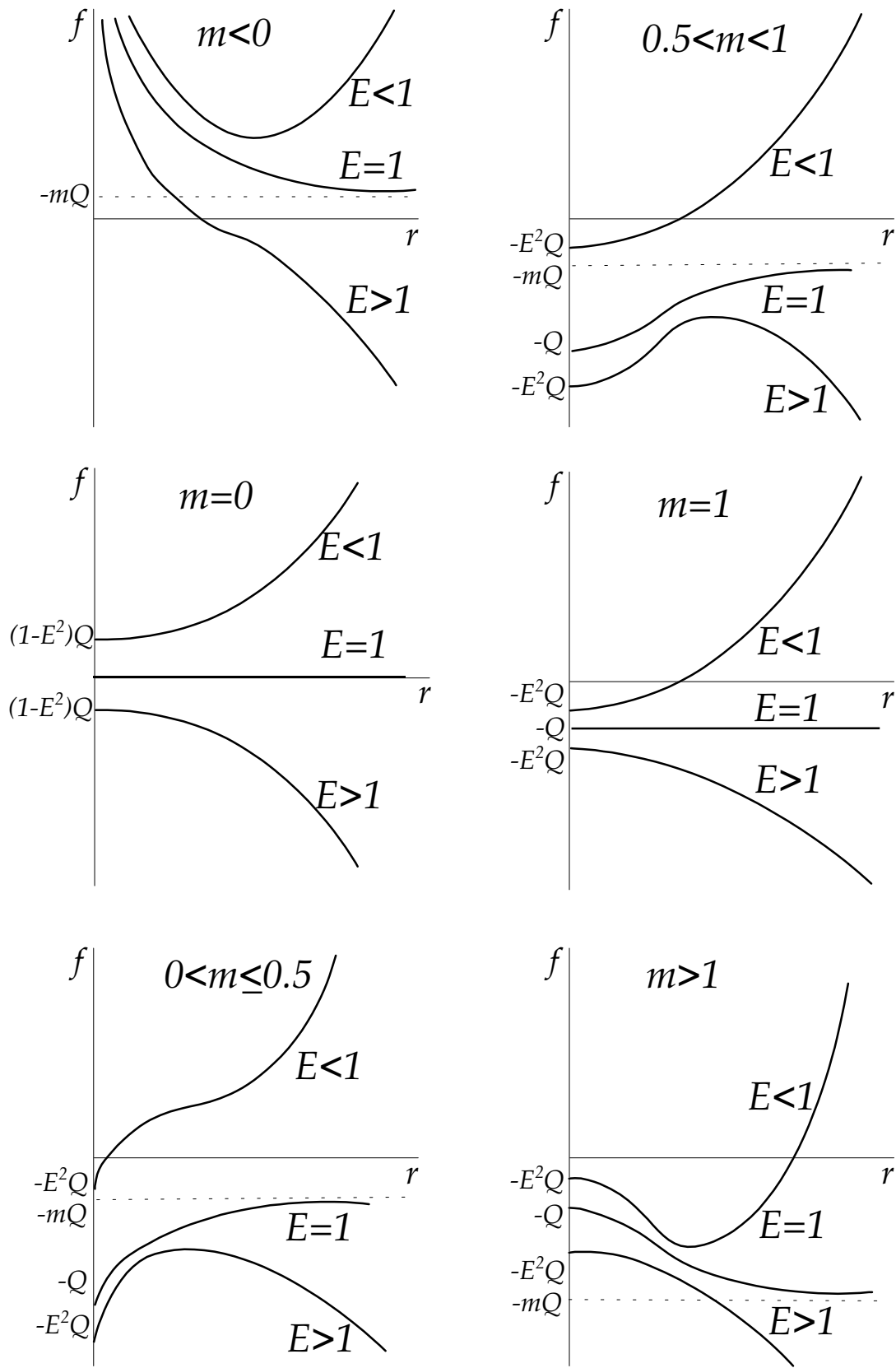
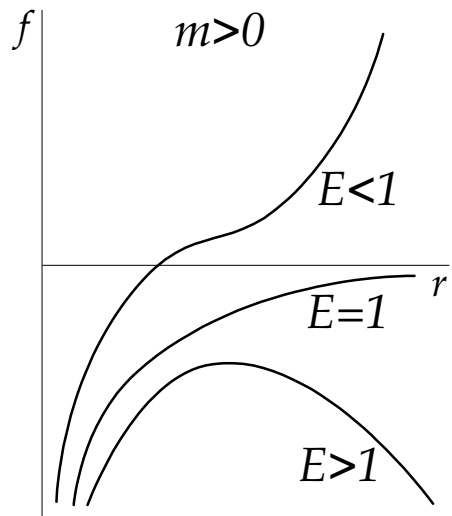
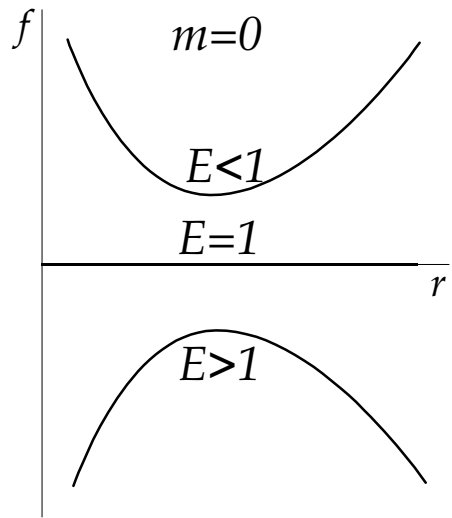
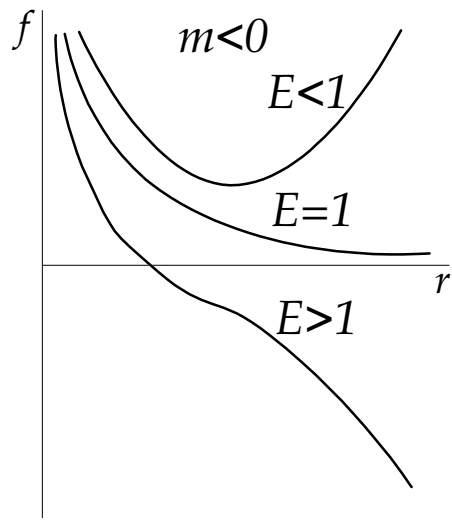


Fig.5

$M \geq 5$



**Fig.6**